Simplified Spatial Correlation Models for Clustered MIMO Channels With Different Array Configurations

Antonio Forenza, *Member, IEEE*, David J. Love, *Member, IEEE*, and Robert W. Heath, Jr., *Senior Member, IEEE*

***Abstract*—An approximate spatial correlation model for clustered multiple-input multiple-output (MIMO) channels is proposed in this paper. The two ingredients for the model are an approximation for uniform linear and circular arrays to avoid numerical integrals and a closed-form expression for the correlation coefficients that is derived for the Laplacian azimuth angle distribution. A new performance metric to compare parametric and nonparametric channel models is proposed and used to show that the proposed model is a good fit to the existing parametric models for low angle spreads (i.e., smaller than 10°). A computational-complexity analysis shows that the proposed method is a numerically efficient way of generating the spatially correlated MIMO channels.**

***Index Terms*—Channel capacity, circular arrays, correlation, linear arrays, multipath channels, multiple-input multiple-output (MIMO) systems.**

I. Introduction

MULTIPLE-INPUT multiple-output (MIMO) communication technology offers a spatial degree of freedom that can be leveraged to achieve significant capacity gains as well as improved diversity advantage [1], [2]. While the theoretical properties of MIMO communication systems have been acknowledged for some time, only now is a pragmatic perspective of MIMO communication in realistic propagation channels being developed [3]–[11]. These results show that realistic MIMO channels have significant spatial correlation due to the clustering of scatterers in the propagation environment. Unfortunately, spatial correlation generally has an adverse effect on capacity and error rate performance [3], [12]. Simulating realistic correlated channels is thus essential to predict the performance of real MIMO systems.

Spatially correlated MIMO channels are typically derived under certain assumptions about the scattering in the propagation environment. One popular correlation model, which we call the clustered channel model, assumes that groups of scatterers are modeled as clusters located around the transmit and receive antenna arrays. Clustered channel models have been validated through measurements [13], [14], and variations have been adopted in different standards such as the IEEE 802.11n Technical Group [15], for wireless local area networks, and the 3GPP Technical Specification Group [16], for third generation cellular systems.

There are two popular approaches to simulate the correlated MIMO channels based on methods derived from single-input multiple-output channel models (see [17] and the references therein). The first one is a parametric approach, which generates the MIMO channel matrix based on a geometrical description of the propagation environment (i.e., ray-tracing techniques). The second one is a nonparametric method, where the spatial correlation across MIMO channels is reproduced by a suitable choice of transmit and receive spatial correlation matrices. Parametric models (PMs) are used to predict the performance of MIMO communication systems in realistic propagation environments, since they describe accurately the spatial characteristics of wireless links. Non-PMs (NPMs) (e.g., the Kronecker model [3], [8]) are defined using a reduced set of channel parameters [i.e., angle spread (AS) and mean angle of arrival (AOA)/departure (AOD)] and are suitable for theoretical analysis of the correlated MIMO channels.

In theoretical analyses of MIMO systems, it may be desirable to study capacity and error rate performance accounting for spatial-correlation effects, due to the propagation channel and the transmit/receive arrays. For this purpose, the channel spatial correlation has to be expressed in closed form as a function of channel and array parameters. In [18], exact expressions of the spatial correlation coefficients were derived for the different spatial distributions (i.e., uniform, Gaussian, and Laplacian) of AOD/AOA for uniform linear arrays (ULAs). This solution, however, is expressed in terms of sums of Bessel functions and does not show a direct dependence of the spatial correlation on the channel/array parameters.

Manuscript received September 22, 2004; revised February 16, 2006 and July 25, 2006. The work of R. W. Heath, Jr. was supported in part by the Office of Naval Research under Grant N00014-05-1-0169 and in part by the National Science Foundation under Grant CCF-514194. The work of D. J. Love was supported in part by the SBC Foundation and in part by the National Science Foundation under Grant CCF0513916. This paper was presented in part at the IEEE Semiannual Vehicular Technolog Conference, Milan, Italy, May 2004. The review of this paper was coordinated by Prof. C. Xiao.

A. Forenza is with Rearden, LLC, San Francisco, CA 94107 USA (e-mail: antonio@rearden.com).

D. J. Love is with the School of Electrical and Computer Engineering, Purdue University, West Lafayette, IN 47907 USA (e-mail: djlove@ecn.purdue.edu).

R. W. Heath, Jr. is with Wireless Networking and Communications Group, Department of Electrical and Computer Engineering, University of Texas at Austin, Austin, TX 78712-0240 USA (e-mail: rheath@ece.utexas.edu).

Color versions of one or more of the figures in this paper are available online at http://ieeexplore.ieee.org.

Digital Object Identifier 10.1109/TVT.2007.897212

In this paper, we propose new closed-form expressions of the spatial correlation matrices in the clustered MIMO channels. We assume a Laplacian distribution of the AOA/AOD, which has been demonstrated to be a good fit for the power angular spectrum [19]–[22] and is practically used by different standards channel models [15], [16], [23]. The key insight is that a small angle approximation, which holds for moderate ASs (i.e., less than $\sim 10^\circ$), allows us to derive a closed-form solution for the spatial-correlation function. Using our method, we can avoid the numerical integration in [18] and can easily obtain the correlation as a function of AS and arrivals. We develop these results for the commonly used ULA and extend these results to the uniform circular array (UCA), which is perhaps the next most common array geometries for future generation access points. To validate our model, we compare it against the existing parametric and nonparametric channel models. To make the comparison, we propose a novel distance metric, which is derived from the mutual information of the MIMO channel, to evaluate the relative performance of parametric and nonparametric channel models. Then, we evaluate this metric in different propagation conditions and show that, for ASs lower than $\sim 10^\circ$, our model is a good fit to the more realistic PMs.

Besides the analytical tractability, another main benefit of the proposed method versus the existing channel models, as we demonstrate, is a reduction in computational complexity and, thus, computation time required to compute the spatial correlation matrices. Because the spatial correlation matrices are a function of the cluster size and location, which are often modeled as random, system level simulations will require averaging over many correlation realizations. For example, in the context of network simulators, where many users and channels need to be simulated [24]–[31], and in detailed propagation studies of the effect of correlation [32], [33], the computational burden to simulate the spatially correlated MIMO channels is a relevant issue. Our proposed channel model enables network simulations with significant computational saving, on the order of 10 to 1000 times compared to the existing methods.

This paper is organized as follows. In Section II, we provide some background on the clustered MIMO channel models as well as the parametric and NPMs. Then, in Section III, we present the analytical derivation of the proposed model for ULA and UCA antenna configurations, outlining the approximation used. In Section IV, we propose a new performance metric to evaluate the relative performance of parametric and nonparametric channel models and show the performance degradation of our method due to the approximation used. Section V describes the computational-complexity analysis of different channel models. Finally, in Section VI, we give some remarks on the applicability of our model in practical system simulators. Concluding remarks are given in Section VII.

II. Description of Clustered Channel Models

In this section, we provide some background on clustered channel models as well as the parametric and NPMs used in our analysis.

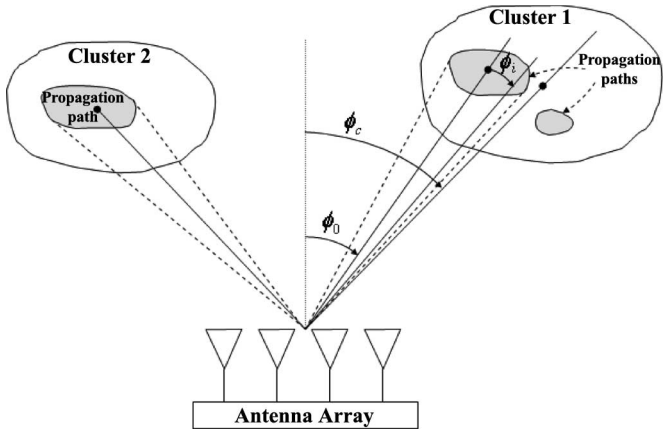

Fig. 1. Geometry of the model representing clusters and propagation paths. The angles ϕ_c and ϕ_0 are the mean AOAs of the cluster and propagation paths, respectively. The angle ϕ_i is the AOA offset of the path.

A. Background and Model Description

One common technique for modeling multipath propagation in indoor environments is the Saleh–Valenzuela model [13], [34], where waves arriving from similar directions and delays are grouped into clusters. Using this method, a mean AOA or AOD is associated with each cluster, and the AOAs/AODs of the subpaths within the same cluster are assumed to be distributed according to a certain probability density function (pdf). The pdf of the AOAs/AODs is chosen to fit the empirically derived angular distribution of the AOAs/AODs or power angular spectrum of the channel. Note that, although the AOAs/AODs are physically distributed over the 3-D space, it has been proven through channel measurements that most of the energy is localized over the azimuth directions [23]. Therefore, we assume the AOAs/AODs to be distributed according to a certain power azimuth spectrum (PAS). The size of a cluster is measured by the cluster AS that is defined as the standard deviation of the PAS.

A graphical representation of the clustered channel model is given in Fig. 1. Without loss of generality, we focus on modeling the receiver spatial correlation. Multiple scatterers around the receive array are modeled as clusters. We use the angle ϕ_{c} to denote the mean AOA/AOD of one cluster. Within the same cluster, each propagation path is characterized by an AOA ϕ_0 and is generated according to a certain PAS. Depending on the system bandwidth, the excess delay across different paths may not be resolvable. In this case, multiple AOAs/AODs are defined with an offset ϕ_i that is relative to the mean AOA/AOD of the propagation path (ϕ_0). In typical channel models for indoor environments [15], the propagation paths within the same clusters are generated with the same mean AOA/AOD as the cluster, and we assume $\phi_0 = \phi_{\mathrm{c}}$.

Several distributions have been proposed thus far to approximate the empirically observed PAS: the nth power of a cosine function and uniform distributions [35]–[37], the Gaussian pdf [38], and the Laplacian pdf [20]–[22], [34], [39]–[41]. Through recent measurement campaigns in indoor [21], [22], [34], [40] and outdoor [19], [20], [39] environments, it has been shown

that the PAS is accurately modeled by the truncated Laplacian pdf, which is given by

$$P_\phi(\phi) = \begin{cases} \frac{\beta}{\sqrt{2}\sigma_\phi} \cdot e^{-|\sqrt{2}\phi/\sigma_\phi|}, & \text{if } \phi \in [-\pi, \pi) \\ 0, & \text{otherwise} \end{cases} \quad (1)$$

where ϕ is the random variable describing the AOA/AOD offset with respect to the mean angle ϕ_0, σ_ϕ is the standard deviation (rms) of the PAS, and $\beta = 1/(1 - e^{-\sqrt{2}\pi/\sigma_\phi})$ is the normalization factor needed to make the function integrate to one. The Laplacian pdf is also used by different standard bodies as in [15], [16], and [23].

We consider a MIMO communication link with M_t transmit and M_r receive antennas. Suppose that the system is wideband and operating in an indoor environment that is accurately modeled using the clustered channel model. Under this assumption, the channel consists of multiple sample taps, which are associated with different clusters. Because the transmitted signals are bandlimited, it is sufficient to model only the discrete-time impulse response (see, e.g., [42])

$$\mathbf{H}[t] = \sum_{\ell=0}^{L-1} \mathbf{H}_\ell[t]\delta[t-\ell] \quad (2)$$

obtained from sampling the band-limited continuous-time impulse response where t denotes the discrete-time index, L is the number of effectively nonzero channel taps (corresponding to the channel clusters), $\delta[t-\ell]$ is the Kronecker delta function,[1] and $\mathbf{H}_\ell[t]$ is the $M_\mathrm{r} \times M_\mathrm{t}$ channel matrix for the ℓth tap. We assume that the taps are uncorrelated; thus, we focus on modeling each channel tap. Hereafter, we briefly describe two common methods to generate the MIMO channel matrices $\mathbf{H}_\ell$.[2]

B. Parametric Channel Model

In parametric channel models, the entries of the MIMO channel matrix are expressed as a function of the channel spatial parameters. The ℓth matrix tap $\mathbf{H}_\ell$ is given by [43] and [11][3]

$$\mathbf{H}_\ell = \frac{1}{\sqrt{N}} \sum_{i=1}^{N} \alpha_i \mathbf{a}_\mathrm{r}\left(\phi_{\ell,i}^\mathrm{r}\right) \mathbf{a}_\mathrm{t}^\dagger\left(\phi_{\ell,i}^\mathrm{t}\right) \quad (3)$$

where N is the number of rays per cluster, α_i is the complex Rayleigh channel coefficient, $\phi_{\ell,i}^\mathrm{t}$ and $\phi_{\ell,i}^\mathrm{r}$ are the AOD and AOA, respectively, of the ith ray within the ℓth cluster, generated according to the Laplacian pdf in (1). Moreover, $\mathbf{a}_\mathrm{t}$ and $\mathbf{a}_\mathrm{r}$ are the transmit and receive array responses, respectively, which are given by

$$\mathbf{a}_\mathrm{t}\left(\phi_{\ell,i}^\mathrm{t}\right) = \left[1, e^{j\Phi_1\left(\phi_{\ell,i}^\mathrm{t}\right)}, \ldots, e^{j\Phi_{(M_\mathrm{t}-1)}\left(\phi_{\ell,i}^\mathrm{t}\right)}\right]^T \quad (4)$$

$$\mathbf{a}_\mathrm{r}\left(\phi_{\ell,i}^\mathrm{r}\right) = \left[1, e^{j\Phi_1\left(\phi_{\ell,i}^\mathrm{r}\right)}, \ldots, e^{j\Phi_{(M_\mathrm{r}-1)}\left(\phi_{\ell,i}^\mathrm{r}\right)}\right]^T \quad (5)$$

where Φ_m is the phase shift of the mth array element with respect to the reference antenna. Note that the expression of Φ_m varies depending on the array configuration and is a function of the AOA/AOD. Equation (3) can be written in closed form as [44, p. 31]

$$\mathbf{H}_\ell = \mathbf{A}_{\mathrm{r},\ell}\mathbf{H}_\alpha\mathbf{A}_{\mathrm{t},\ell}^\dagger \quad (6)$$

where $\mathbf{A}_{\mathrm{t},\ell} = [\mathbf{a}_\mathrm{t}(\phi_{\ell,1}), \ldots, \mathbf{a}_\mathrm{t}(\phi_{\ell,N})]$, $\mathbf{A}_{\mathrm{r},\ell} = [\mathbf{a}_\mathrm{r}(\phi_{\ell,1}), \ldots, \mathbf{a}_\mathrm{r}(\phi_{\ell,N})]$, and $\mathbf{H}_\alpha = 1/\sqrt{N}\mathrm{diag}(\alpha_1, \ldots, \alpha_N)$. We define the channel covariance matrix for the ℓth tap as

$$\mathbf{R}_{H,\ell} = \mathcal{E}\left[\mathrm{vec}(\mathbf{H}_\ell)\mathrm{vec}(\mathbf{H}_\ell)^\dagger\right]. \quad (7)$$

C. Nonparametric Channel Model

We use the Kronecker model to describe the stochastic evolution of each matrix tap $\mathbf{H}_\ell$ as [3]

$$\mathbf{H}_\ell = \mathbf{R}_{\mathrm{r},\ell}^{1/2}\mathbf{H}_w\mathbf{R}_{\mathrm{t},\ell}^{T/2} \quad (8)$$

where $\mathbf{H}_w$ is a $M_\mathrm{r} \times M_\mathrm{t}$ matrix whose entries are independently distributed according to the complex Gaussian distribution. Moreover, $\mathbf{R}_{\mathrm{t},\ell}$ and $\mathbf{R}_{\mathrm{r},\ell}$ are the spatial correlation matrices at the transmitter and receiver, respectively, which express the correlation of the receive/transmit signals across the array elements. The channel covariance matrix of the NPM in (8) is given by the Kronecker product of the transmit and receive correlation matrices as

$$\mathbf{R}_{H,\ell} = \mathbf{R}_{\mathrm{t},\ell} \otimes \mathbf{R}_{\mathrm{r},\ell}. \quad (9)$$

In the clustered channel model, the coefficients of $\mathbf{R}_\mathrm{t}$ and $\mathbf{R}_\mathrm{r}$[4] for a single channel tap are characterized by a certain AS and AOA. Since the same method is used to calculate each correlation matrix, we will use the notation $\mathbf{R}$ to refer to both the transmit or receive correlation matrix. Likewise, we will use M, instead of M_r or M_t, to indicate the number of antennas. The (m, n) entry of the matrix $\mathbf{R}$ for spaced array configurations is defined as [18], [39]

$$\mathbf{R}_{m,n} = \int_{-\pi}^{\pi} e^{j[\Phi_m(\phi) - \Phi_n(\phi)]} P_\phi(\phi) d\phi \quad (10)$$

where $P_\phi(\phi)$ is the Laplacian pdf in (1), and the term $\Phi_m(\phi) - \Phi_n(\phi)$ accounts for the phase difference between the mth and nth array element due to spacing.

[1] The Kronecker delta is defined as

$$\delta[t-\ell] = \begin{cases} 1, & \text{if } t = \ell \\ 0, & \text{otherwise.} \end{cases}$$

[2] We omit the $[t]$ notation for simplicity as normally, the coherence of the channel implies that it is constant over many symbol periods.

[3] We use $\mathcal{C}N(0,1)$ to denote a random variable with real and imaginary parts that are independent identically distributed (i.i.d.) according to $N(0, 1/2)$, * to denote conjugation, ^{T} to denote transposition, † to denote conjugation and transposition, $|\cdot|$ to denote the absolute value, $\|\cdot\|_1$ to denote the 1-norm, $\langle\cdot,\cdot\rangle$ to denote the complex vector space inner product, $\mathrm{vec}(\cdot)$ to denote the vec-operator of matrices, and $\mathcal{E}[\cdot]$ to denote the expected value of random variables.

[4] We omit the subscript ℓ because we focus on a single tap.

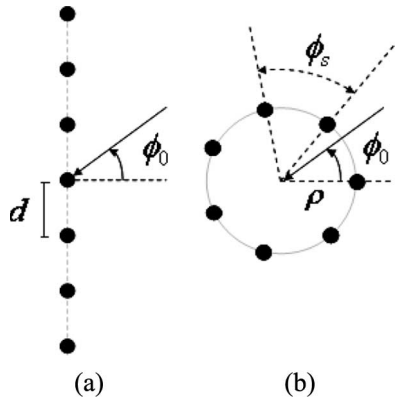

Fig. 2. ULA and UCA configurations, seven-element case. (a) ULA. (b) UCA.

III. Proposed Model of the Spatial Correlation Matrix

In this section, we derive an approximate expression of the spatial correlation matrices $\mathbf{R}$ reported in (8) for a single channel tap. We will show how to derive the closed form of $\mathbf{R}$ under an approximation for low ASs for both ULA and UCA configurations depicted in Fig. 2.

A. Uniform Linear Array (ULA)

We express the phase shift in (10) of the mth array element with respect to the reference antenna as a function of the AOA as

$$\Phi_m(\phi) = kdm\sin(\phi_0 - \phi) \tag{11}$$

where $m = 0, \ldots, M-1$, ϕ is the AOA offset with respect to the mean AOA of the cluster ϕ_0, and k is the wavenumber. Substituting (11) in (10), we express the cross-correlational coefficient of the ULA as

$$\mathbf{R}_{m,n} = \int_{-\pi}^{\pi} e^{jkd(m-n)\sin(\phi_0-\phi)} P_\phi(\phi)d\phi \tag{12}$$

where $P_\phi(\phi)$ is the pdf given in (1).

Let us express the exponent of the function inside the integral as

$$\sin(\phi_0 - \phi) = \sin\phi_0\cos\phi - \cos\phi_0\sin\phi. \tag{13}$$

Expanding with a first-order Taylor series (assuming $\phi \approx 0$)

$$\sin(\phi_0 - \phi) \approx \sin\phi_0 - \phi\cos\phi_0. \tag{14}$$

Substituting (14) into (12), we get

$$\mathbf{R}_{m,n} \approx e^{jkd(m-n)\sin\phi_0} \cdot \int_{-\pi}^{\pi} e^{-jkd(m-n)\cos(\phi_0)\phi} P_\phi(\phi)d\phi. \tag{15}$$

From (1), we observe that the truncated Laplacian PAS is zero outside the range $[-\pi, \pi)$. Therefore, the integration of $P_\phi(\phi)$ truncated over $[-\pi, \pi)$ is approximately equivalent to the integration over the real line. Then, substituting (1) into (15), we get

$$[\mathbf{R}(\phi_0, \sigma_\phi)]_{m,n} \approx e^{jkd(m-n)\sin\phi_0} \cdot \int_{-\infty}^{\infty} e^{-jkd(m-n)\cos(\phi_0)\phi} \frac{\beta}{\sqrt{2}\sigma_\phi} e^{-|\sqrt{2}\phi/\sigma_\phi|}d\phi. \tag{16}$$

Equation (16) consists of the product of a complex exponential term times an integral term. The integral term is the characteristic function of the Laplacian pdf in (1), and it can be expressed as

$$[\mathbf{B}(\phi_0, \sigma_\phi)]_{m,n} = \int_{-\infty}^{\infty} e^{-jkd(m-n)\cos(\phi_0)\phi} \frac{\beta}{\sqrt{2}\sigma_\phi} e^{-|\sqrt{2}\phi/\sigma_\phi|}d\phi = \mathcal{F}_\omega\left\{\frac{\beta}{\sqrt{2}\sigma_\phi} e^{-|\sqrt{2}\phi/\sigma_\phi|}\right\} \tag{17}$$

where $\mathcal{F}_\omega$ denotes the Fourier transform evaluated at $\omega = kd(m-n)\cos\phi_0$. Solving (17), we get

$$[\mathbf{B}(\phi_0, \sigma_\phi)]_{m,n} = \frac{\beta}{1 + \frac{\sigma_\phi^2}{2} \cdot [kd(m-n)\cos\phi_0]^2} \tag{18}$$

with $m, n = 0, \ldots, (M-1)$. Therefore, substituting (18) in (16), we derive the following closed form for the correlation coefficients across all the array elements:

$$[\mathbf{R}(\phi_0, \sigma_\phi)]_{m,n} \approx \frac{\beta e^{jkd(m-n)\sin\phi_0}}{1 + \frac{\sigma_\phi^2}{2} \cdot [kd(m-n)\cos\phi_0]^2}. \tag{19}$$

The complex exponential term in (16) can be written as

$$e^{jkd(m-n)\sin\phi_0} = e^{jkdm\sin\phi_0} \cdot e^{-jkdn\sin\phi_0} \tag{20}$$

where the multiplicative factors at the right-hand side of (20) are the entries of the steering vector of the ULA, which are given by

$$\mathbf{a}_{\text{ula}}(\phi_0) = \left[1, e^{jkd\sin\phi_0}, \ldots, e^{jkd(M-1)\sin\phi_0}\right]^T. \tag{21}$$

Using the definition in (21), we derive the spatial correlation matrix, with complex entries given by (19) as

$$\mathbf{R}(\phi_0, \sigma_\phi) \approx \left[\mathbf{a}_{\text{ula}}(\phi_0) \cdot \mathbf{a}_{\text{ula}}^\dagger(\phi_0)\right] \odot \mathbf{B}(\phi_0, \sigma_\phi) \tag{22}$$

where $\odot$ denotes the Shur–Hadamard (or elementwise) product, and $\mathbf{a}(\phi_0)$ is the array response (column vector) for the mean azimuth AOA (ϕ_0). A similar result was given in [45] and [46], where the Gaussian distribution was used for the PAS. In our case, however, we computed the matrix $\mathbf{R}(\phi_0, \sigma_\phi)$ for the case of Laplacian pdf, which is given by (1).

B. Uniform Circular Array (UCA)

We express the phase shift in (10) of the mth array element with respect to the center of the UCA as a function of the AOA as

$$\Phi_m(\phi) = k\rho\cos\left[(\phi_0 - \phi) - \phi_m\right]. \tag{23}$$

Substituting (23) in (10), we write

$$\mathbf{R}_{m,n} = \int_{-\pi}^{\pi} e^{jk\rho[\cos(\phi_0-\phi_m-\phi)-\cos(\phi_0-\phi_n-\phi)]} P_\phi(\phi)d\phi. \tag{24}$$

Consider the exponent in (24)

$$\Phi_{mn} = \cos(\phi_0 - \phi_m - \phi) - \cos(\phi_0 - \phi_n - \phi). \tag{25}$$

Applying the following trigonometric formula of angle addition:

$$\cos(\alpha - \beta) = \cos\alpha\cos\beta + \sin\alpha\sin\beta \tag{26}$$

we find

$$\begin{aligned}\Phi_{mn} = {} & [\cos(\phi_0 - \phi_m) - \cos(\phi_0 - \phi_n)]\cos\phi \\ & + [\sin(\phi_0 - \phi_m) - \sin(\phi_0 - \phi_n)]\sin\phi.\end{aligned} \tag{27}$$

Using the first-order Taylor expansion (assuming $\phi \approx 0$)

$$\begin{aligned}\Phi_{mn} &\approx [\cos(\phi_0 - \phi_m) - \cos(\phi_0 - \phi_n)] \\ &\quad + [\sin(\phi_0 - \phi_m) - \sin(\phi_0 - \phi_n)]\,\phi \\ &= F_{mn} + G_{mn}\phi\end{aligned} \tag{28}$$

where we defined $F_{mn} = \cos(\phi_0 - \phi_m) - \cos(\phi_0 - \phi_n)$ and $G_{mn} = \sin(\phi_0 - \phi_m) - \sin(\phi_0 - \phi_n)$. Substituting these values in (24)

$$\mathbf{R}_{m,n} \approx e^{jk\rho F_{mn}} \cdot \int_{-\infty}^{\infty} e^{jk\rho G_{mn}\phi} P_\phi(\phi)d\phi. \tag{29}$$

Similar to the ULA case, we identify the complex exponential term and the integral term in (29). The integral term can be expressed in terms of the characteristic function of the Laplacian pdf as

$$[\mathbf{B}(\phi_0, \sigma_\phi)]_{m,n} = \mathcal{F}_\omega\left\{\frac{1}{\sqrt{2}\sigma_\phi} e^{-|\sqrt{2}\phi/\sigma_\phi|}\right\} \tag{30}$$

where $\mathcal{F}_\omega$ denotes, as usual, the Fourier transform evaluated at $\omega = -k\rho G_{mn}$. Then

$$\begin{aligned}&[\mathbf{B}(\phi_0, \sigma_\phi)]_{m,n} \\ &= \frac{\beta}{1 + \frac{\sigma_\phi^2}{2}\cdot\left[k\rho\left(\sin(\phi_0 - m\phi_s) - \sin(\phi_0 - n\phi_s)\right)\right]^2}\end{aligned} \tag{31}$$

where we assumed $\phi_m = m\phi_s$ and $\phi_n = n\phi_s$ for UCAs, with $m, n = 0, \ldots, (M-1)$. Substituting (31) in (29) and using the definition of F_{mn} given before, we can write the closed-form solution of the correlation coefficients for the UCA as

$$\begin{aligned}&[\mathbf{R}(\phi_0, \sigma_\phi)]_{m,n} \\ &\approx \frac{\beta e^{jk\rho[\cos(\phi_0 - m\phi_s) - \cos(\phi_0 - n\phi_s)]}}{1 + \frac{\sigma_\phi^2}{2}\cdot\left[k\rho\left(\sin(\phi_0 - m\phi_s) - \sin(\phi_0 - n\phi_s)\right)\right]^2}.\end{aligned} \tag{32}$$

The complex exponential term in (29) may be expanded as

$$e^{jk\rho F_{mn}} = e^{jk\rho\cos(\phi_0 - \phi_m)} \cdot e^{-jk\rho\cos(\phi_0 - \phi_n)}. \tag{33}$$

where each complex exponential at the right-hand side of (33) is the entry of the steering vector of the UCA, which is defined as [47]

$$\begin{aligned}\mathbf{a}_{\text{uca}}(\phi_0) = \Big[&e^{jk\rho\cos(\phi_0)}, e^{jk\rho\cos(\phi_0 - \phi_s)} \\ &\ldots, e^{jk\rho\cos(\phi_0 - (M-1)\phi_s)}\Big]^T\end{aligned} \tag{34}$$

where we used the usual assumption of $\phi_m = m\phi_s$ for uniformly spaced circular arrays. Finally, using (31) and the definition (34)

$$\mathbf{R}(\phi_0, \sigma_\phi) \approx \left[\mathbf{a}_{\text{uca}}(\phi_0) \cdot \mathbf{a}_{\text{uca}}^\dagger(\phi_0)\right] \odot \mathbf{B}(\phi_0, \sigma_\phi)$$

which is the same expression of the spatial correlation matrix as in (22). Note that the closed form of $\mathbf{R}(\phi_0, \sigma_\phi)$ in (22) is the same for both the ULA and the UCA cases. The expressions of the matrix $\mathbf{B}(\phi_0, \sigma_\phi)$ and the vector $\mathbf{a}(\phi_0)$ are different, however, and they are reported, respectively, in (18) and (21) for the ULA case and in (31) and (34) for the UCA case.

IV. Performance Comparison of Different MIMO Channel Models

We compare the performance of the proposed nonparametric channel model against the PMs based on the metrics derived from the MIMO capacity and spatial correlation matrix. From these metrics, we evaluate the conditions under which nonparametric and parametric MIMO channel models provide the same performance. Then, we determine the channel scenarios (defined by different combinations of values of ϕ_0 and σ_ϕ) for which our model provides similar performance as the PMs.

We consider three different models to generate the complex MIMO channel matrix $\mathbf{H}$.

1) PM is described in (3) based on sum of N rays.
2) Exact NPM (ENPM) in (8) employs the exact correlation coefficients derived in [7] for ULAs. In [7], the closed-form expression of the spatial correlation coefficients is expressed as infinite sum of Bessel functions of the first kind. For simulation purposes, we truncate this series to a finite sum of N_{B} Bessel functions.
3) Approximate NPM (ANPM) in (8) uses the approximated spatial correlation coefficients in (19) and (32) for the ULAs and UCAs, respectively.

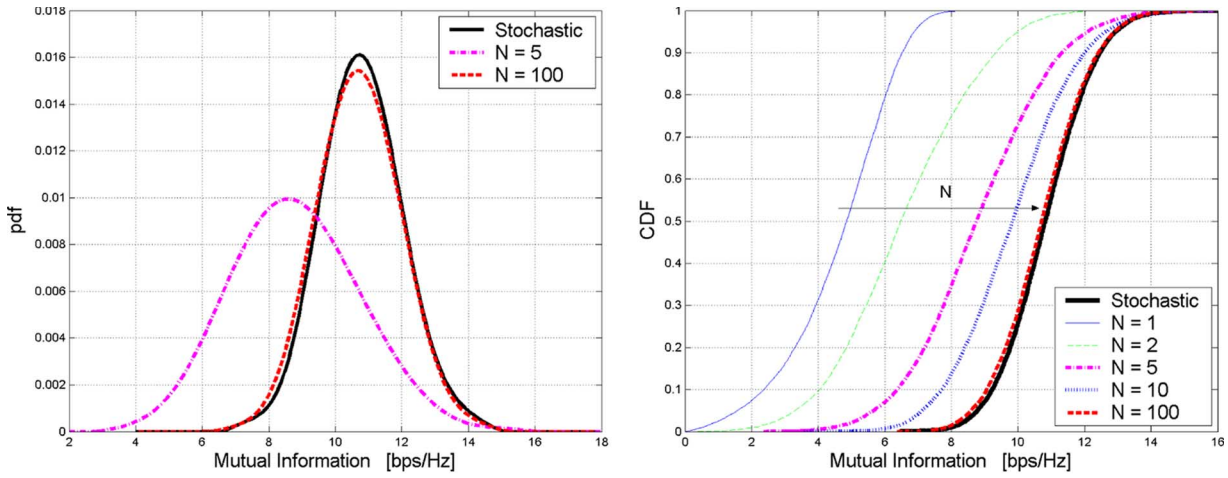

(a) (b)

Fig. 3. PDF and CDF of the mutual information for PM and ENPM with variable number of rays (N). The same number of transmit/receive antennas (i.e., $M_{\rm t} = M_{\rm r} = 4$) and single cluster channel with $\sigma_\phi = 50^\circ$ and $\phi_0 = 0^\circ$ was used. (a) PDF. (b) CDF.

A. Performance Metrics

To compare the relative performance of the channel models described previously, we employ a well-known metric defined from the channel covariance matrix [48]

$$\Psi(\mathbf{R}_1, \mathbf{R}_2) = \frac{\|\mathbf{R}_1 - \mathbf{R}_2\|_{\rm F}}{\|\mathbf{R}_1\|_{\rm F}} \tag{35}$$

where $\mathbf{R}_1$ and $\mathbf{R}_2$ are the spatial correlation matrices obtained from two different models. For the PM, we employ the definition of spatial correlation matrix in (7), whereas for the ENPM and ANPM, we use (9).

We observe that in [49] and [50], the MIMO ergodic capacity was expressed in closed form as a function of the spatial correlation matrix. Hence, the error provided by the metric in (35) is directly related to the mismatch of the ergodic capacity obtained through the two different channel models. The results in [49] and [50], however, are derived for nonparametric channel models employing the Kroneker structure in (8) and cannot be extended, in general, to the PMs in (3) (unless certain assumptions are made on the channel model [3]). Moreover, we note that the covariance matrix in (9) is parametric, whereas (7) is the average of a random matrix, and its estimate may be biased. Fair comparisons of parametric versus nonparametric channel models have to rely on the distribution of the mutual information, which is derived from the MIMO channel matrix (rather than the spatial correlation matrices).

The mutual information of a MIMO channel, assuming equal power allocation across the transmit antennas and Gaussian signaling, is given by

$$C(\mathbf{H}) = \log_2 \left| \mathbf{I}_{M_{\rm r}} + \frac{\gamma_{\rm o}}{M_{\rm t}} \mathbf{H}\mathbf{H}^\dagger \right| \tag{36}$$

where $\gamma_{\rm o}$ is the average signal-to-noise ratio (SNR). From (36), it is possible to derive two metrics that are commonly used to evaluate the performance of MIMO systems: mean and 10% outage capacity [51]. In the correlated MIMO channels, however, the Gaussian approximation [52]–[54] does not always hold (particularly when the channel is high spatially correlated), and the pdf of C cannot be characterized simply by its first- and second-order moments. Hence, we define the following metric derived from the pdf of the mutual information in (36)

$$D_{\rm pdf}(f,g) = \frac{\|f(C) - g(C)\|_1}{\|f(C)\|_1 + \|g(C)\|_1} = \frac{1}{2}\int_0^\infty |f(C) - g(C)|\, dC \tag{37}$$

where $f(C)$ and $g(C)$ are the pdfs of C for different channel models, with $\|f(C)\|_1 = \|g(C)\|_1 = 1$ by the definition of the pdf. Note that (37) satisfies the condition $0 \leq D_{\rm pdf}(f,g) \leq 1$, with $D_{\rm pdf}(f,g) = 0$ when $f(C) = g(C), \forall C$. In the next section, we describe how to estimate the pdf's $f(C)$ and $g(C)$.

In the following results, we choose the PM as the reference to compare the performance of our proposed ANPM, since the PM describes more accurately the physical properties of the propagation channel and can be used to simulate any array configuration. PMs, however, assume a finite number of rays in the propagation environment, as opposed to NPMs for which the multipaths are assumed to be continuously distributed in space. Hence, we begin by comparing the PM against the ENPM for the different numbers of rays (N).

B. Performance Comparison of the PM Against ENPM

Fig. 3(a) shows the pdf of the mutual information in (36) for the PM and ENPM for ULAs, with a variable number of rays (N), $M_{\rm t} = M_{\rm r} = M = 4$, SNR $= 10$ dB, $\sigma_\phi = 50^\circ$, and $\phi_0 = 0^\circ$ both at the transmit and receive sides. In the following results, we assume that the array-element spacing is $d = 0.5\lambda$, with λ being the wavelength. The pdf of C is computed through Monte Carlo simulations over 10 000 channel instances and by curve fitting. Note that the Gaussian approximation can

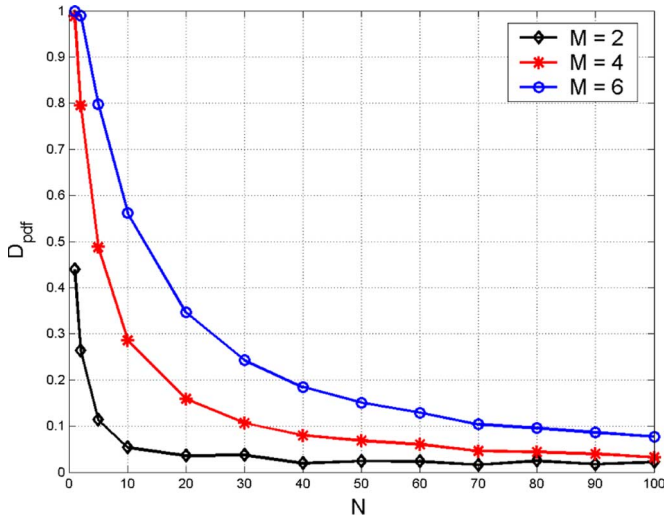

Fig. 4. Distance between the pdf of C as a function of the number of rays for PM and ENPM. The same number of transmit/receive antennas (i.e., $M_{\rm t} = M_{\rm r} = M$) and single cluster channel with AS $\sigma_\phi = 50^\circ$ and $\phi_0 = 0^\circ$ was used.

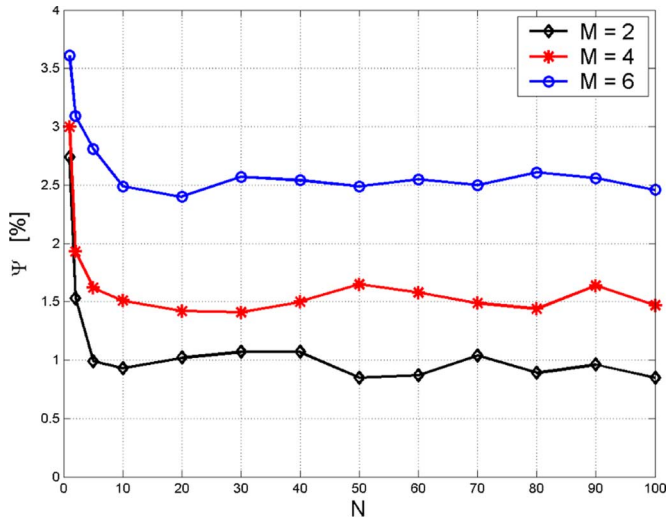

Fig. 5. Distance Ψ between the spatial correlation matrices for PM and ENPM. ULA is assumed with $M_{\rm t} = 4$, $M_{\rm r} = 1$. The channel is simulated with $\phi_0 = 0^\circ$ and different values of σ_ϕ.

be used to fit the pdf of the MIMO channel capacity for the i.i.d. and single-sided spatially correlated channels, as shown in [52]–[54]. We observed, however, that the Gaussian fit becomes loose when the channel spatial correlation is high (i.e., low AS). Since our final goal is to compare the performance of ANPM against PM in any correlated scenario, we employ polynomial fitting functions to approximate the pdf of C. Fig. 3(a) shows that, as the number of rays increases from 5 to 100, the PM approaches the performance of ENPM. Similar results are given in Fig. 3(b) for the cumulative density function (CDF) of the mutual information. We observe that the PM approaches the ENPM for $N \to 100$.

Next, we compute the optimal value of N for which PM converges to ENPM, for different system parameters, by employing the metric in (37). Fig. 4 shows the distance metric in (37) as a function of the number of rays (N) for different numbers of transmit/receive antennas $M_{\rm t} = M_{\rm r} = M$. We compare the performance of the PM with variable N against the ENPM with $N_{\rm B} = 500$. The MIMO channel is simulated with $\sigma_\phi = 50^\circ$ and $\phi_0 = 0^\circ$ both at the transmit and receive sides. We observe that $D_{\rm pdf}$ decreases as N increases, since a larger number of rays for the PM more closely approximate the continuous spatial distribution of rays in the ENPM. Moreover, for fixed N, $D_{\rm pdf}$ increases with M due to the higher dimensionality of the MIMO channel. We empirically choose the threshold of 5% as a target value and observe that, for the practical case of $M = 4$, about 70 rays are enough for the PM to approximate the ENPM. Note that the channel is generated with low spatial correlation (i.e., large AS), and fewer rays may be required for smaller values of σ_ϕ.

Fig. 5 shows the metric in (35) as a function of N, for $M_{\rm t} = M$ and $M_{\rm r} = 1$ in the correlated MIMO channels with $\phi_0 = 0^\circ$ and variable σ_ϕ. The matrix $\mathbf{R}_1$ is generated according to the ENPM in (9), whereas the matrix $\mathbf{R}_2$ is derived from the PM in (7). We choose a target of 10% as in [48]. We observe that, for any N, the PM is a good fit to the ENPM in terms of Ψ, since a single receive antenna is assumed.

C. Performance of the Proposed ANPM Against PM

Here, we compare the performance of the proposed ANPM against PMs for ULAs and UCAs. We consider practical MIMO systems with $M_{\rm t} = M_{\rm r} = 4$ antennas, and we simulate the PM with $N = 100$ rays. Moreover, we use the same channel parameters (i.e., σ_ϕ and ϕ_0) both at the transmit and receive sides. Note that we choose $N = 100$ to guarantee that the PM fits the NPMs also for the large AS (i.e., 30°). For the small ASs and number of antennas, however, the PM also fits NPMs for the smaller values of N, as shown in Fig. 4.

Fig. 6(a) shows the metric in (36) as a function of the channel parameters for ULAs. We observe that, for values of AS lower than 10° and for any value of mean AOA in the range $[0^\circ, 90^\circ]$, $D_{\rm pdf}$ is always below the predefined 5% target. Then, for these values of σ_ϕ and ϕ_0, the ANPM approaches the performance of PM. Similarly, Fig. 6(b) shows that the range of values for which the ANPM with UCAs approximates the PM within the 5% target of $D_{\rm pdf}$ is $\phi_0 \in [0^\circ, 90^\circ]$ and $\sigma_\phi \leq 5^\circ$.

Fig. 7(a) and (b) shows the metric in (35) as a function of the channel parameters for both ULAs and UCAs. Once more, the ANPM approximates the PM within the 10% target of Ψ for any value of ϕ_0 and for σ_ϕ below 10° and 5° for the ULA and UCA, respectively. We conclude that the proposed ANPM for ULAs and UCAs is a good approximation to the PM for small ASs (i.e., lower than $\sim 10^\circ$ for ULAs).

V. Computational-Complexity Analysis

Hereafter, we analyze the computational cost of the three channel models described previously and evaluate the complexity reduction of the ANPM over the PM and ENPM. In this analysis, we count the number of arithmetic functions used to compute the MIMO complex channel coefficients in (2), with $t = 1, \ldots, N_{\rm s}$ and $N_{\rm s}$ being the number of channel instances to be simulated. We assume that any arithmetic function has computational cost of K, while recognizing that the value of K is machine dependent.

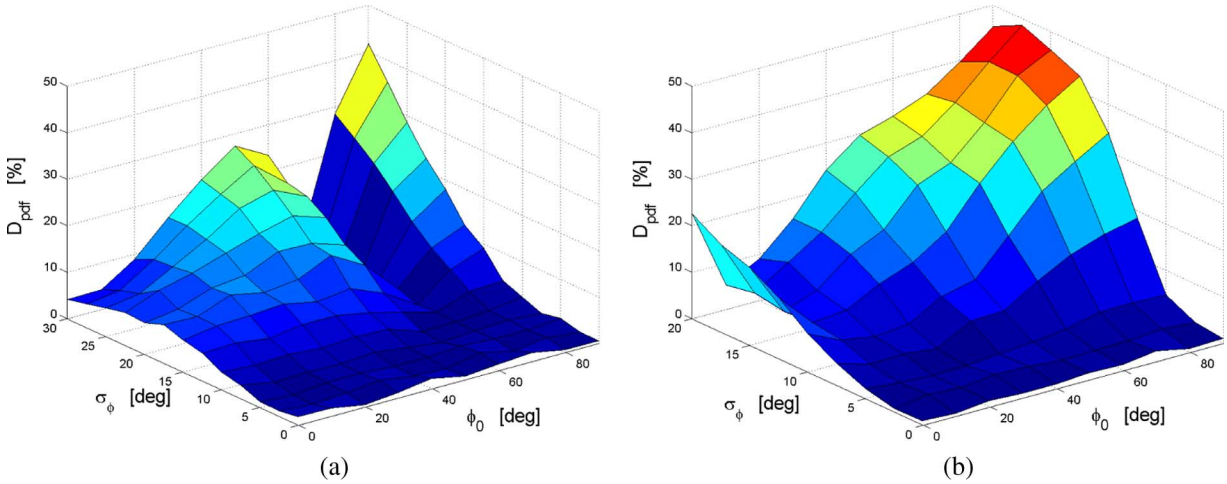

Fig. 6. Distance between the pdf of Ω as a function of AS and mean AOA for PM and ANPM. The same number of transmit/receive antennas (i.e., $M_{\rm t} = M_{\rm r} = M = 4$) is assumed with ULA and UCA. (a) ULA. (b) UCA.

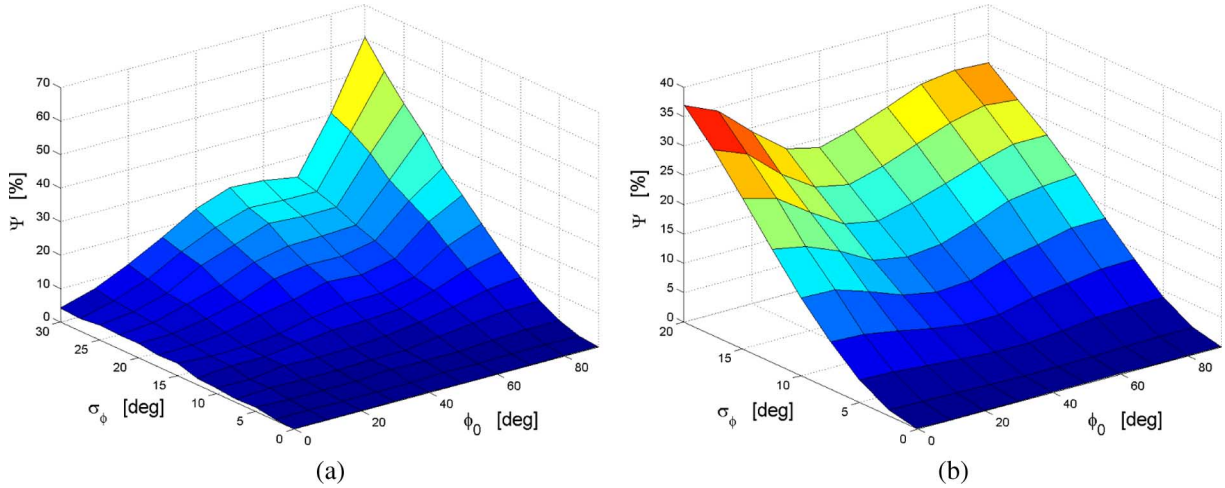

Fig. 7. Distance Ψ between the spatial correlation matrices for PM and ANPM. The same number of transmit/receive antennas (i.e., $M_{\rm t} = M_{\rm r} = M = 4$) with ULA and UCA. (a) ULA. (b) UCA.

We first consider the case of ULA. For the PM, the cost to evaluate the ℓth matrix tap in (3) is $N(6N+5)(M_{\rm t}+M_{\rm r})K$. When L clusters are simulated, with $N_{\rm s}$ samples each, the total computational complexity of PM is

$$\Omega_{\rm PM} = N_{\rm s}LN(6N+5)(M_{\rm t}+M_{\rm r})K. \tag{38}$$

For the ENPM, we use the approximation for Bessel functions of the first kind in [18], truncating the infinite series to the order $N_{\rm B}$. To numerically compute the Bessel functions from the order zero up to $2N_{\rm B}+1$, we employ a well-known method based on polynomial approximation and backward recurrence [55]. It is possible to show that the cost to compute the complex entries of the matrices $\mathbf{R}_{{\rm t},\ell}$ and $\mathbf{R}_{{\rm r},\ell}$ in (8) for the L channel clusters is given by $\Omega_{\rm R,ENPM} = \mathcal{O}(62N_{\rm B}L(M_{\rm t}^2+M_{\rm r}^2)K)$, for $N_{\rm B} \gg L$. Moreover, the cost for Cholesky decomposition of the transmit/receive correlation matrices is $\Omega_{\rm chol} = \mathcal{O}(2/3L(M_{\rm t}^3+M_{\rm r}^3)K)$, and the matrix multiplication for the Kronecker model in (8) has complexity $\Omega_{\rm mult} = \mathcal{O}(N_{\rm s}L(6M_{\rm t}^2M_{\rm r}+M_{\rm t}M_{\rm r}^2)K)$. Then, we derive the computational cost of the ENPM as

$$\Omega_{\rm ENPM} = \Omega_{\rm R,ENPM} + \Omega_{\rm chol} + \Omega_{\rm mult}. \tag{39}$$

The ANPM evaluates the transmit/receive correlation matrices through the closed-form expression in (19) with the computational effort $\Omega_{\rm R,ANPM} = \mathcal{O}(20L(M_{\rm t}^2+M_{\rm r}^2)K)$, while $\Omega_{\rm chol}$ and $\Omega_{\rm mult}$ are the same as for the ENPM. Then, the total computational complexity of ANPM is

$$\Omega_{\rm ANPM} = \Omega_{\rm R,ANPM} + \Omega_{\rm chol} + \Omega_{\rm mult}. \tag{40}$$

We now use these results to evaluate the computational saving of the ANPM over the PM and ENPM. To make our discussion concrete, we consider the case of multiuser MIMO systems with $M_{\rm t} = M$ transmit antennas and U users with $M_{\rm r} = 1$ receive antenna each. For these systems, the computational burden to generate spatial channels for all the users may be very high, particularly when U is a large number.

Hereafter, we demonstrate the significant complexity reduction attainable through the ANPM. From (38) and (40), we derive the computational gain of ANPM against PM as

$$G_{\mathrm{ANPM-PM}} = \frac{\Omega_{\mathrm{PM}} \cdot U}{\Omega_{\mathrm{ANPM}} \cdot U} \approx \frac{N^2}{M} \tag{41}$$

where we assumed $N \gg 1$. Equation (41) reveals that the computational gain of ANPM depends essentially on the number of rays used for the PM, given that $N \gg M$. For example, we consider the practical case of $M = 4$, and we assume $N = 70$, for which PMs approximate NPMs within the 5% target of D_{pdf}, as shown in Fig. 4. Under these assumptions, the computational saving of ANPM over PM to calculate the MIMO channel matrix taps is $G_{\mathrm{ANPM-PM}} \approx 1200$.

Similarly, from (39) and (40), we compute the gain produced by the ANPM over the ENPM as

$$G_{\mathrm{ANPM-ENPM}} = \frac{\Omega_{\mathrm{ENPM}} \cdot U}{\Omega_{\mathrm{ANPM}} \cdot U} \approx \frac{10N_{\mathrm{B}}}{N_{\mathrm{s}}} + 1 \tag{42}$$

where we assumed $N_{\mathrm{s}} \gg M$. Assuming $N_{\mathrm{B}} = 100$ as in the IEEE 802.11n standard channel model [56] and $N_{\mathrm{s}} = 100$, we derive the computational gain of the ANPM over ENPM as $G_{\mathrm{ANPM-ENPM}} \approx 10$.

For the case of UCA, we observe that the computational complexity of the PM is the same as for ULA, since the same number of arithmetic functions is used to calculate the steering vectors in (21) and (34). Moreover, the ANPM computes the spatial correlation matrices using the proposed closed form in (32) with computational complexity $\Omega_{\mathrm{R,ANPM}} = \mathcal{O}(26L(M_{\mathrm{t}}^2 + M_{\mathrm{r}}^2)K)$. Therefore, the gain of ANPM over PM for the UCA case is the same as in (41).

VI. Remarks on Applicability of the ANPM

We observed that the approximation for small angles employed by the ANPM limits this model to be used only for channel scenarios characterized by small AS (i.e., $\leq 10^\circ$ for ULAs). Channel models for outdoor environments for cellular systems typically assume that the AS of each tap at the base station is on the order of 5°. Some examples are the 3GPP spatial channel model [16] and the COST-259 model [23]. One practical application of the proposed ANPM is to generate the spatially correlated channels for the MIMO broadcast channel with multiple transmit antennas and single receive antenna per user.

Moreover, we showed that the ANPM provides closed-form expressions of the correlation coefficients as a function of the channel parameters (i.e., AS and mean AOA) for ULAs and UCAs. These expressions are the useful tools to analyze the performance of different arrays exploiting space diversity in the clustered MIMO channel models. For example, in [57], we used the ANPM to compare the performance of space versus pattern diversity techniques in the spatially correlated MIMO channels.

VII. Conclusion

We proposed the closed-form expressions for generating the spatial correlation matrices for the clustered MIMO channel models. Our approach assumes a Laplacian PAS and uses a small angle approximation to obtain a closed-form solution for the spatial correlation matrix that is valid for either ULAs or circular arrays. Despite its simple analytical tractability, the proposed method fits more complex (but more exact) methods proposed in the literature for the ASs less than 10°, thereby reducing the computational complexity to simulate the correlated MIMO channels. The proposed method is a computationally efficient solution for network simulators, where the spatially correlated MIMO channels have to be simulated for a large number of users.

References

[1] D. Gesbert, M. Shafi, D.-S. Shiu, P. J. Smith, and A. Naguib, "From theory to practice: An overview of MIMO space-time coded wireless systems," *IEEE J. Sel. Areas Commun.*, vol. 21, no. 3, pp. 681–683, Jun. 2003.

[2] A. Goldsmith, S. A. Jafar, N. Jindal, and S. Vishwanath, "Capacity limits of MIMO channels," *IEEE J. Sel. Areas Commun.*, vol. 21, no. 5, pp. 684–702, Jun. 2003.

[3] D.-S. Shiu, G. J. Foschini, M. J. Gans, and J. M. Kahn, "Fading correlation and its effect on the capacity of multielement antenna systems," *IEEE Trans. Commun.*, vol. 48, no. 3, pp. 502–513, Mar. 2000.

[4] D. Chizhik, F. Rashid-Farrokhi, J. Ling, and A. Lozano, "Effect of antenna separation on the capacity of BLAST in correlated channels," *IEEE Commun. Lett.*, vol. 4, no. 11, pp. 337–339, Nov. 2000.

[5] J. Fuhl, A. F. Molisch, and E. Bonek, "Unified channel model for mobile radio systems with smart antennas," *Proc. Inst. Electr. Eng.—Radar, Sonar Navigation*, vol. 145, no. 1, pp. 32–41, Feb. 1998.

[6] J. W. Wallace and M. A. Jensen, "Modeling the indoor MIMO wireless channel," *IEEE Trans. Antennas Propag.*, vol. 50, no. 5, pp. 591–599, May 2002.

[7] J. P. Kermoal, L. Schumacher, P. E. Mogensen, and K. I. Pedersen, "Experimental investigation of correlation properties of MIMO radio channels for indoor picocell scenarios," in *Proc. IEEE VTC*, Sep. 2000, vol. 1, pp. 14–21.

[8] J. P. Kermoal, L. Schumacher, K. I. Pedersen, P. E. Mogensen, and F. Frederiksen, "A stochastic MIMO radio channel model with experimental validation," *IEEE J. Sel. Areas Commun.*, vol. 20, no. 6, pp. 1211–1226, Aug. 2002.

[9] C. Oestges, V. Erceg, and A. J. Paulraj, "A physical scattering model for MIMO macrocellular broadband wireless channels," *IEEE J. Sel. Areas Commun.*, vol. 21, no. 5, pp. 721–729, Jun. 2003.

[10] D. S. Baum, D. Gore, R. Nabar, S. Panchanathan, K. V. S. Hari, V. Erceg, and A. J. Paulraj, "Measurement and characterization of broadband MIMO fixed wireless channels at 2.5 GHz," in *Proc. IEEE Conf. Pers. Wireless Commun.*, Dec. 2000, pp. 203–206.

[11] A. F. Molisch, "A generic model for MIMO wireless propagation channels in macro- and microcells," *IEEE Trans. Signal Process.*, vol. 52, no. 1, pp. 61–71, Jan. 2004.

[12] D. Gore, R. Heath, and A. Paulraj, "Statistical antenna selection for spatial multiplexing systems," in *Proc. IEEE Int. Conf. Commun.*, Apr. 2002, vol. 1, pp. 450–454.

[13] A. A. M. Saleh and R. A. Valenzuela, "A statistical model for indoor multipath propagation," *IEEE J. Sel. Areas Commun.*, vol. SAC-5, no. 2, pp. 128–137, Feb. 1987.

[14] J. W. Wallace and M. A. Jensen, "Statistical characteristics of measured MIMO wireless channel data and comparison to conventional models," in *Proc. IEEE Veh. Technol. Conf.*, Oct. 2001, vol. 2, pp. 1078–1082. no. 7–11.

[15] V. Erceg *et al.*, *TGn Channel Models*, May 2004, IEEE 802.11-03/940r4.

[16] "Spatial channel model, SCM-134 text V6.0," *Spatial Channel Model AHG (Combined ad-hoc from 3GPP and 3GPP2)*, Apr. 2003.

[17] R. B. Ertel, P. Carderi, K. W. Sowerby, T. S. Rappaport, and J. H. Reed, "Overview of spatial channel models for antenna array communication systems," in *Proc. IEEE Conf. Pers. Wireless Commun.*, Feb. 1998, pp. 10–22.

[18] L. Schumacher, K. I. Pedersen, and P. E. Mogensen, "From antenna spacings to theoretical capacities—Guidelines for simulating MIMO

systems," in *Proc. IEEE Int. Symp. Pers., Indoor, Mobile Radio Commun.*, Sep. 2002, vol. 2, pp. 587–592.
[19] K. I. Pedersen, P. E. Mogensen, and B. H. Fleury, "Power azimuth spectrum in outdoor environments," *Electron. Lett.*, vol. 33, no. 18, pp. 1583–1584, Aug. 1997.
[20] K. I. Pedersen, P. E. Mogensen, and B. H. Fleury, "A stochastic model of the temporal and azimuthal dispersion seen at the base station in outdoor propagation environments," *IEEE Trans. Veh. Technol.*, vol. 49, no. 2, pp. 437–447, Mar. 2000.
[21] Q. H. Spencer, B. D. Jeffs, M. A. Jensen, and A. L. Swindlehurst, "Modeling the statistical time and angle of arrival characteristics of an indoor multipath channel," *IEEE J. Sel. Areas Commun.*, vol. 18, no. 3, pp. 347–360, Mar. 2000.
[22] G. German, Q. Spencer, L. Swindlehust, and R. Valenzuela, "Wireless indoor channel modeling: Statistical agreement of ray tracing simulations and channel sounding measurements," in *Proc. IEEE Int. Conf. Acoust., Speech, Signal Process.*, May 2001, vol. 4, pp. 2501–2504.
[23] L. M. Correia, *Wireless Flexible Personalised Communications*. New York: Wiley, 2001.
[24] J. Wigard and P. Mogensen, "A simple mapping from C/I to FER and BER for a GSM type of air-interface," in *Proc. IEEE Int. Symp. Pers., Indoor, Mobile Radio Commun.*, Oct. 1996, vol. 1, pp. 78–82.
[25] H. Olofsson, M. Almgren, C. Johansson, M. Hook, and F. Kronestedt, "Improved interface between link level and system level simulations applied to GSM," in *Proc. IEEE 6th Int. Conf. Universal Pers. Commun. Rec.*, Oct. 1997, vol. 1, pp. 79–83.
[26] J. Wigard, T. T. Nielsen, P. H. Michaelsen, and P. Mogensen, "BER and FER prediction of control and traffic channels for a GSM type of air-interface," in *Proc. IEEE Veh. Technol. Conf.*, May 1998, vol. 2, pp. 1588–1592.
[27] C. Caini and G. Riva, "A new vector quantization technique for performance evaluation in frequency hopping mobile radio systems," *IEEE Commun. Lett.*, vol. 4, no. 8, pp. 252–254, Aug. 2000.
[28] R. J. Punnoose, P. V. Nikitin, and D. D. Stancil, "Efficient simulation of Ricean fading within a packet simulator," in *Proc. IEEE Veh. Technol. Conf.*, Sep. 2000, vol. 2, pp. 764–767.
[29] D. J. Mazzarese and W. A. Krzymien, "High throughput downlink cellular packet data access with multiple antennas and multiuser diversity," in *Proc. IEEE Veh. Technol. Conf.*, Apr. 2003, vol. 2, pp. 1079–1083.
[30] M. Pukkila, G. P. Mattellini, and P. A. Ranta, "Constant modulus single antenna interference cancellation for GSM," in *Proc. IEEE Veh. Technol. Conf.*, May 2004, vol. 1, pp. 584–588.
[31] P. A. Ranta, H. Berg, E. Tuomaala, and Z. Uykan, "Dual antenna diversity reception for EGPRS terminals," in *Proc. IEEE Veh. Technol. Conf.*, May 2004, vol. 1, pp. 510–514.
[32] M. Dohler, J. Dominguez, and H. Aghvami, "Link capacity analysis for virtual antenna arrays," in *Proc. IEEE Veh. Technol. Conf.*, Sep. 2002, vol. 1, pp. 440–443.
[33] A. Kastrisios, M. Dohler, and H. Aghvami, "Influence of channel characteristics on the performance of VAA with deployed STBCs," in *Proc. IEEE Veh. Technol. Conf.*, Apr. 2003, vol. 2, pp. 1138–1142.
[34] Q. Spencer, M. Rice, B. Jeffs, and M. Jensen, "A statistical model for angle of arrival in indoor multipath propagation," in *Proc. IEEE Veh. Technol. Conf.*, May 1997, vol. 3, pp. 1415–1419.
[35] W. C. Y. Lee, "Effects on the correlation between two mobile radio base-station antennas," *IEEE Trans. Commun.*, vol. COM-21, no. 11, pp. 1214–1224, Nov. 1973.
[36] W. C. Jakes, *Microwave Mobile Communications*. Piscataway, NJ: IEEE Press, 1974.
[37] J. Salz and J. H. Winters, "Effect of fading correlation on adaptive arrays in digital mobile radio," *IEEE Trans. Veh. Technol.*, vol. 43, no. 4, pp. 1049–1057, Nov. 1994.
[38] M. T. Feeney and J. D. Parsons, "Cross-correlation between 900 MHz signal received on vertically separated antennas in small-cell radio systems," *Proc. Inst. Electr. Eng. I*, vol. 138, no. 2, pp. 81–86, Apr. 1991.
[39] K. I. Pedersen, P. E. Mogensen, and B. H. Fleury, "Spatial channel characteristics in outdoor environments and their impact on BS antenna system performance," in *Proc. IEEE Veh. Technol. Conf.*, 1998, vol. 2, pp. 719–723.
[40] A. S. Y. Poon and M. Ho, "Indoor multiple-antenna channel characterization from 2 to 8 GHz," in *Proc. IEEE Int. Conf. Commun.*, May 2003, vol. 5, pp. 3519–3523.
[41] R. J. Cramer, R. A. Scholtz, and M. Z. Win, "Evaluation of an ultra-wideband propagation channel," *IEEE Trans. Antennas Propag.*, vol. 50, no. 5, pp. 561–570, May 2002.
[42] H. Bölcskei, M. Borgmann, and A. J. Paulraj, "Impact of the propagation environment on the performance of space-frequency coded MIMO-OFDM," *IEEE J. Sel. Areas Commun.*, vol. 21, no. 3, pp. 427–439, Apr. 2003.
[43] M. Stege, J. Jelitto, M. Bronzel, and G. Fettweis, "A multiple input-multiple output channel model for simulation of Tx- and Rx-diversity wireless systems," in *Proc. IEEE Veh. Technol. Conf.*, Sep. 2000, vol. 2, pp. 833–839.
[44] K. Yu, "Multiple-input multiple-output radio propagation channels: Characteristics and models," Ph.D dissertation, KTH Dept. Signals, Sens., Syst., Stockholm, Sweden, 2005.
[45] B. Ottersten, "Spatial division multiple access (SDMA) in wireless communications," in *Proc. Nordic Radio Symp. Signal Process.*, 1995.
[46] B. Ottersten, "Array processing for wireless communications," in *Proc. 8th IEEE Signal Process. Workshop Statistical Signal and Array Process.*, Mar. 1996, pp. 466–473.
[47] A. Forenza and R. W. Heath, Jr., "Impact of antenna geometry on MIMO communication in indoor clustered channels," in *Proc. IEEE Antennas Propag. Symp.*, Jun. 2004, vol. 2, pp. 1700–1703.
[48] K. Yu, M. Bengtsson, B. Ottersten, D. McNamara, P. Karlsson, and M. Beach, "Modeling of wide-band MIMO radio channels based on NLOS indoor measurements," *IEEE Trans. Veh. Technol.*, vol. 53, no. 3, pp. 655–665, May 2004.
[49] M. Kiessling and J. Speidel, "Mutual information of MIMO channels in correlated Rayleigh fading environments—A general solution," in *Proc. IEEE Int. Conf. Commun.*, Jun. 2004, vol. 2, pp. 814–818.
[50] A. Forenza, M. R. McKay, A. Pandharipande, R. W. Heath, Jr., and I. B. Collings, "Adaptive MIMO transmission for exploiting the capacity of spatially correlated channels," *IEEE Trans. Veh. Technol.*, vol. 56, no. 2, pp. 619–630, Mar. 2007.
[51] A. Paulraj, R. Nabar, and D. Gore, *Introduction to Space-Time Wireless Communications*. New York: Cambridge Univ. Press, 2003.
[52] P. J. Smith and M. Shafi, "On a Gaussian approximation to the capacity of wireless MIMO systems," in *Proc. IEEE Int. Conf. Commun.*, Apr. 2002, vol. 1, pp. 406–410.
[53] P. J. Smith, S. Roy, and M. Shafi, "Capacity of MIMO systems with semicorrelated flat fading," *IEEE Trans. Inf. Theory*, vol. 49, no. 10, pp. 2781–2788, Oct. 2003.
[54] P. J. Smith and M. Shafi, "An approximate capacity distribution for MIMO systems," *IEEE Trans. Commun.*, vol. 52, no. 6, pp. 887–890, Jun. 2004.
[55] S. Zhang and J. Jin, *Computation of Special Functions*. New York: Wiley, 1996.
[56] L. Schumacher, *WLAN MIMO Channel Matlab Program*. [Online]. Available: http:\\www.info.fundp.ac.be\~lsc\Research\IEEE_80211_HTSG_CMSC\distribution_terms.html
[57] A. Forenza and R. W. Heath, Jr., "Benefit of pattern diversity via 2-element array of circular patch antennas in indoor clustered MIMO channels," *IEEE Trans. Commun.*, vol. 54, no. 5, pp. 943–954, May 2006.

Antonio Forenza (S'04–M'06) received the M.S. degree in telecommunications engineering from the Politecnico di Torino, Torino, Italy, and the Eurecom Institute, Sophia Antipolis, France, in 2001 and the Ph.D. degree in electrical and computer engineering from the University of Texas at Austin in 2006.

He was a Systems Engineer Intern at Iospan Wireless, Inc., San Jose, CA, which is a start-up company that developed the first commercial multiple-input multiple-output (MIMO) orthogonal frequency-division multiplexing communication system, in 2001. He was a Systems Research Engineer at ArrayComm, Inc., San Jose, in Fall 2001, where he was actively involved in the design and implementation of smart antenna systems for the 3G wireless platform. Over the summers of 2004 and 2005, he was a Research Engineer Intern at the Samsung Advanced Institute of Technology, Suwon, Korea, and at Freescale Semiconductor, Inc., Austin, respectively, developing adaptive MIMO transmission and multiuser MIMO precoding techniques for the 3GPP, IEEE 802.11n, and IEEE 802.16e standards systems. Since June 2006, he has been with Rearden, LLC, San Francisco, CA, as a Senior Systems Engineer. His main research focus was on link adaptation and physical layer algorithm design. His research interests include MIMO antenna design, adaptive MIMO transmission techniques, precoding methods for multiuser MIMO, and smart antenna signal processing.

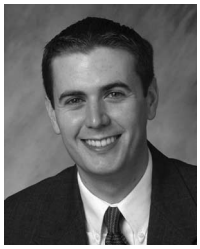

David J. Love (S'98–M'05) was born in Garland, TX. He received the B.S. (with highest honors), M.S.E., and Ph.D. degrees in electrical engineering from the University of Texas at Austin in 2000, 2002, and 2004, respectively.

During the summers of 2000 and 2002, he was with the Texas Instruments DSPS R&D Center, Dallas, TX. Since August 2004, he has been with the School of Electrical and Computer Engineering, Purdue University, West Lafayette, IN, as an Assistant Professor. His research interests are in the design and analysis of communication systems, coding theory, and information theory.

Dr. Love is a member of Tau Beta Pi and Eta Kappa Nu. In 2003, he received the IEEE Vehicular Technology Society Daniel Noble Fellowship.

Robert W. Heath, Jr. (S'96–M'01–SM'06) received the B.S. and M.S. degrees in electrical engineering from the University of Virginia, Charlottesville, in 1996 and 1997, respectively, and the Ph.D. degree in electrical engineering from Stanford University, Stanford, CA, in 2002.

From 1998 to 2001, he was a Senior Member of the Technical Staff and then a Senior Consultant at Iospan Wireless Inc., San Jose, CA, where he worked on the design and implementation of the physical and link layers of the first commercial multiple-input multiple-output (MIMO) orthogonal frequency-division multiplexing communication system. In 2003, he founded the MIMO Wireless Inc., which is a consulting company dedicated to the advancement of MIMO technology. Since January 2002, he has been in the Department of Electrical and Computer Engineering, University of Texas at Austin, where he is currently an Assistant Professor and a member of the Wireless Networking and Communications Group. His research interests cover a broad range of MIMO communication, including antenna design, practical receiver architectures, limited feedback techniques, *ad hoc* networking, and scheduling algorithms, as well as 60-GHz communication techniques.

Dr. Heath serves as an Editor for the IEEE TRANSACTIONS ON COMMUNICATION, is a former Associate Editor for the IEEE TRANSACTIONS ON VEHICULAR TECHNOLOGY, and is a member of the Signal Processing for Communications Technical Committee of the IEEE Signal Processing Society.